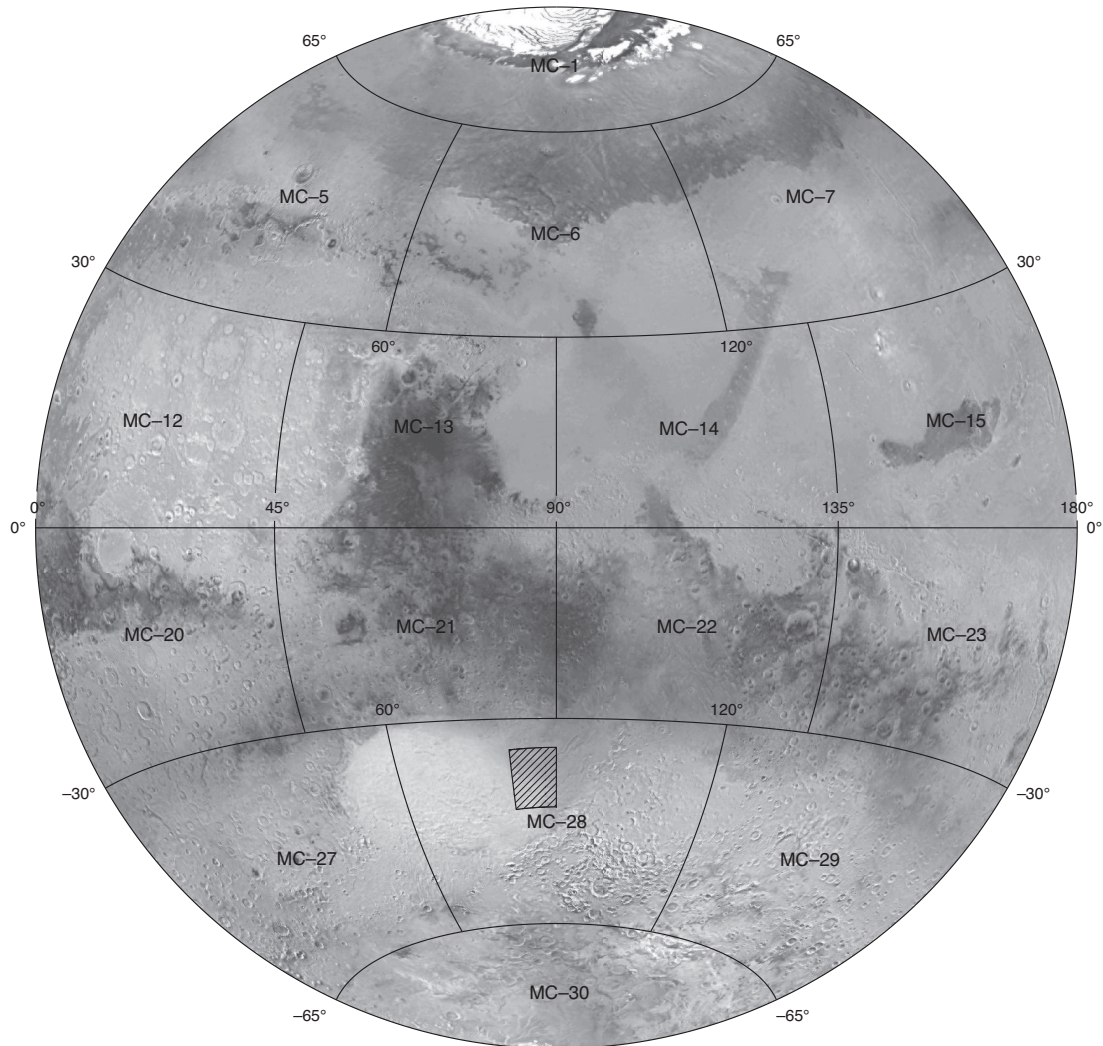


Prepared for the National Aeronautics and Space Administration

Geologic Map of MTM -40277, -45277, -40272, and -45272 Quadrangles, Eastern Hellas Planitia Region of Mars

By Leslie F. Bleamaster III and David A. Crown

Pamphlet to accompany
Scientific Investigations Map 3096



2010

U.S. Department of the Interior
U.S. Geological Survey

Contents

Introduction	1
Regional Geology and History	1
Data and Methods	2
Crater Counting Methodology	3
Stratigraphy	3
Hellas Rim Assemblage	3
Hellas Floor Assemblage	5
Vallis and Channel Materials	5
Crater Materials	6
Discussion	6
Fluvial Systems that dissect the Hellas Rim	6
Extensions of Dao and Harmakhis Valles onto the Basin Floor and Contributions to Hellas Planitia from the Rim	7
Boundary between the East Hellas Basin Rim and Hellas Planitia	7
Geologic History	8
Acknowledgments	8
References Cited	8

Table

1. Areas, crater densities, relative ages, and contact relations for map units in the eastern Hellas Planitia region of Mars	11
---	----

Introduction

Hellas Planitia comprises the floor deposits of the Hellas basin, more than 2,000 km across and 8 km deep, which is located in the southern hemisphere's cratered highlands and is the largest well-preserved impact structure on the Martian surface (fig. 1). The circum-Hellas highlands represent a significant percentage of the southern hemisphere of Mars and have served as a locus for volcanic and sedimentary activity throughout Martian geologic time. Hellas basin topography has had a long-lasting influence, acting as Mars' deepest and second largest depositional sink, as a source for global dust storms (Greeley and others, 1992), and as a forcing agent on southern hemisphere atmospheric circulation (Colaprete and others, 2004, 2005). The region lies in the Martian mid-latitude zone where geomorphic indicators of past, and possibly contemporary, ground ice are prominent (Greeley and Guest, 1987; Crown and others, 1992; Squyres and others, 1992; Leonard and Tanaka, 2001; Mest and Crown, 2001; Mustard and others, 2001; Crown and others, 2005; Berman and others, 2009). The highlands north of the basin show concentrations of Noachian valley networks (Carr, 1996), and those to the east show prominent lobate debris aprons that are considered to be geomorphic indicators of ground ice (Squyres, 1979, 1989; Lucchitta, 1984; Squyres and Carr, 1986; Pierce and Crown, 2003; Chuang and Crown, 2005). Several studies have proposed that Hellas itself was the site of extensive glacial and lacustrine activity (Kargel and Strom, 1992; Moore and Wilhelms, 2001, 2007; Crown and others, 2005; Wilson and others, 2007). Recent analyses of mineralogical information from Mars Express' OMEGA (Observatoire pour la Minéralogie, l'Eau les Glaces et l'Activité) and Mars Reconnaissance Orbiter's CRISM (Compact Reconnaissance Imaging Spectrometer for Mars) reveal outcrops of hydrated phyllosilicates in the region (Mustard and others, 2007; Pelkey and others, 2007), strengthening an already strong case for past aqueous activity in and around Hellas basin.

Our mapping and evaluation of landforms and materials of the Hellas region from basin rim to floor provides further insight into Martian global climate regimes and into the abundance, distribution, and flux of volatiles through history. Mars Transverse Mercator (MTM) quadrangles -40277, -45277, -45272, and -40272 (lat 37.5° S.-47.5° S., long 270° W.-280° W.) cover the eastern portion of the Hellas basin including the boundary between its floor and rim, the distal portions of Dao and Harmakhis Valles, and the deposits of eastern Hellas Planitia. The geologic mapping, at 1:1,000,000-scale from Viking Orbiter, Thermal Emission Imaging System (THEMIS) infrared (IR) and visible (VIS) wavelength, and Mars Orbiter Camera (MOC) narrow-angle images, combined with Mars Orbiter Laser Altimeter (MOLA) topographic data, characterizes the geologic materials and processes that have shaped this region. In particular, the mapping helps to evaluate landforms and deposits resulting from modification of highland terrains by volatile-driven degradation. This mapping study builds on previous mapping in Hellas Planitia and to the east (Crown and others, 1992; Tanaka and Leonard, 1995; Greeley and Guest, 1987; Price, 1998; Leonard and Tanaka, 2001; Mest and Crown, 2001, 2002, 2003,

2006; Crown and Greeley, 2007) and facilitates comparisons between the geologic history of the east rim, the remainder of the rim, and Hellas Planitia. Specific objectives of our mapping are (1) to reconstruct fluvial systems that dissect the Hellas rim, (2) to characterize the extensions of Dao and Harmakhis Valles onto the basin floor and to identify, if present, sediments these canyons contributed to Hellas Planitia from the rim, and (3) to investigate the mode of origin, age, and history of modification of the boundary between the east rim and Hellas Planitia.

Regional Geology and History

The general geology of the Hellas region is known from 1:15,000,000-scale, Viking-based geologic mapping of the eastern equatorial region of Mars (Greeley and Guest, 1987) and earlier Mariner 9-based mapping efforts (Potter, 1976; Scott and Carr, 1978). Later studies of Hellas have included updated mapping of the entire basin at 1:5,000,000 scale (Tanaka and Leonard, 1995; Leonard and Tanaka, 2001). Hellas basin and the surrounding highlands exhibit landforms shaped by a diversity of geologic processes, preserve exposures of Noachian, Hesperian, and Amazonian units, and extend across a wide range in latitude and elevation. Formation of Hellas basin by impact in the Early Noachian Epoch resulted in widely distributed ejecta materials and upheaved crust, which provided the precursor materials/surfaces of the rugged rim terrain (Leonard and Tanaka, 2001). Broad-scale, plan-form asymmetry of Hellas basin has been recognized, and oblique impact remains a popular speculative hypothesis for its general shape (Leonard and Tanaka, 2001 and references therein); however, asymmetry also may result from subsequent, localized basin modification unrelated to the initial impact. The Argyre impact partly blanketed the western rim of Hellas with ejecta and may have been the source of several medium-sized secondary impacts in the region between Hellas and Argyre basin and across Hellas Planitia (Morrison and Frey, 2007). Subsequent impacts on the Hellas basin rim, and within Hellas Planitia, resurfaced local regions with impact breccias and may have controlled the locations of later volcanic and tectonic centers (Schultz, 1984; Schultz and Frey, 1990).

Once broad-scale basin topography stabilized, Hellas was subject to infilling by aeolian, fluvial, glacial, and volcanic materials. Pyroclastic volcanism in the Late Noachian and Early Hesperian Epochs formed Tyrrhena and Hadriaca Paterae on the northeast Hellas basin rim, as well as Amphitrites and Peneus Paterae on the south rim (Peterson, 1977, 1978; Greeley and Spudis, 1981; Greeley and Crown, 1990; Crown and Greeley, 1993). Subsequent effusive volcanism created lava flows southwest of Tyrrhena Patera and may have triggered early development of Dao and Harmakhis Valles along Hellas' northeast rim (Squyres and others, 1987; Crown and others, 1992; Tanaka and others, 2002). Wrinkle ridges deform lavas and sedimentary materials that were emplaced within Hellas basin, in Malea Planum, and in Hesperia Planum. The Amazonian Period is characterized by morphologies and deposits indicative of (1) widespread aeolian processes that eroded the Hellas rim and deposited smooth materials in local catchments in central Hellas

Planitia, (2) mass wasting and debris flows that form large aprons around rim massifs and along steep interior basin scarps, and (3) dune fields, yardangs, dust-devil tracks, and transient splotches; interior basin fines are actively being moved and removed by aeolian transport mechanisms (Moore and Edgett, 1993; Leonard and Tanaka, 2001). In southern regions ($> \text{lat } 40^\circ \text{ S}$), the terrain is blanketed by mid-latitude mantling deposits considered to be a vast contemporary (last few millions of years) reservoir of volatiles (Mustard and others, 2001), which could play a major role in the formation of youthful gullies on crater and canyon walls (Bleamaster and Crown, 2005) and overall crater degradation (Berman and others, 2005, 2009).

The basin-floor materials in the map area are included in widespread plains material previously mapped across the entire basin and generally attributed to a combination (typically unspecified) of volcanic, sedimentary, and aeolian materials dissected and redistributed by fluvial activity and modified by the wind (Potter, 1976; Greeley and Guest, 1987; Crown and others, 1992; Moore and Edgett, 1993; Tanaka and Leonard, 1995; Price, 1998; Leonard and Tanaka, 2001). Additional interpretations of the geology of the basin interior from older datasets include widespread glaciation (Kargel and Strom, 1992; see also Baker and others, 1991). In Viking Orbiter images, wrinkle ridges, mesas, and channels are evident in the basin interior, and high-resolution images reveal layering in several local scarps and benches within the hummocky floor terrain. Tanaka and Leonard (1995) favor an aeolian-dominated environment for the basin interior. More recently, Moore and Wilhelms (2001, 2007), citing evidence from MOC images primarily of the deepest parts of western Hellas Planitia (below $-6,900 \text{ m}$), suggested that Hellas basin contained ice-covered lakes. Accordingly, they attributed layered sediments and polygonal cavities to a lacustrine environment. Viking and MOLA data suggest shorelines at $-6,900 \text{ m}$, $-5,800 \text{ m}$, and $-3,100 \text{ m}$ (fig. 2) (Moore and Wilhelms, 2001, 2007). Crown and others (2005), citing highland crater preservation, proposed the $-1,800 \text{ m}$ contour as a potential maximum high-stand for a Hellas paleolake. Leverington and Ghent (2004) modeled crustal rebound in response to the removal of large bodies of water from the surface of Mars; Hellas basin was one of their candidate sites. This rebound may have induced sufficient lithospheric stress to deform the Hellas floor materials, giving the central plateau the ridged and hummocky appearance preserved today.

Maps of Dao/Niger, Harmakhis, and Reull Valles (Price, 1998; Mest and Crown, 2002, 2003) show evidence for small, young, integrated watersheds adjacent to remnants of the cratered highlands, large expanses of sedimentary plains surrounding the canyons, and a concentration of Amazonian debris aprons shed from massifs, crater rims, and canyons walls. Viking image analyses showed numerous small channels in the plains adjacent to Dao/Niger and Harmakhis Valles and a sequence of plains adjacent to Reull Vallis that was attributed to progressive degradation of the adjacent highlands and (or) flooding and subsequent erosion from Reull Vallis. Several of these previously defined units extend into the current map area. Regional syntheses of the geology of eastern Hellas based on Viking MTM mapping provide constraints on the nature and sequences of volatile-driven processes from the Noachian to

the Amazonian Period (Greeley and Crown, 1990; Crown and others, 1992; Mest and Crown, 2001; Crown and others, 2005).

Data and Methods

Digital files in raster and vector format produced by the U.S. Geological Survey (USGS) were used in the geological mapping of the eastern Hellas Planitia region in conjunction with Geographic Information Systems (GIS) software. Datasets used include a mixed-resolution ($>231 \text{ m/pixel}$) Viking Orbiter Mars Transverse Mercator (MTM) base mosaic, full-resolution THEMIS day- and night-time IR ($\sim 100 \text{ m/pixel}$) and VIS ($\sim 20 \text{ m/pixel}$) wavelength image strips (data through March 2005), 128 pixel/degree ($\sim 463 \text{ m/pixel}$) resolution MOLA derived digital elevation model (DEM), grayscale synthetic hillshades, surface slope maps, and a 200-m -interval contour shapefile. Additional datasets used in our mapping and crater counts include a publicly released THEMIS daytime IR mosaic in simple cylindrical projection resampled to a resolution of 256 pixel/degree ($\sim 231 \text{ m/pixel}$) and individually processed MOC narrow-angle images at resolutions better than 12 m/pixel . The publicly released IR mosaic contains image data released subsequent to production of the USGS base materials. MOC images were used in selected areas to supply detailed morphologic information and to discern the distribution of finely layered deposits, which are resolved only in higher-resolution images.

The Viking, THEMIS, and MOLA DEM data were all processed using the Integrated Software for Imagers and Spectrometers (ISIS) software produced and distributed by the USGS Astrogeology Team (<http://isis.astrogeology.usgs.gov>). Map-projected THEMIS images were produced from individual raw, radiometrically calibrated data acquired from Arizona State University (<http://themis-data.asu.edu>). All of the digital data, with the exception of THEMIS IR mosaic, are in Transverse Mercator map projection with a center longitude of 270° and a center latitude of 0° using the International Astronomical Union (IAU) 2000 shape model of Mars (Seidelmann and others, 2002). All of the USGS digital data were produced in a format that could easily be imported into a GIS.

This project took advantage of advances in digital technologies utilizing Environmental Systems Research Institute (ESRI) ArcGIS ArcView 9.0 software for georeferencing and 3D analysis of datasets; however, geological mapping was conducted primarily on a merged data product including the Viking MTM mosaic/colored MOLA DEM with superposed THEMIS VIS images in Adobe Illustrator. The THEMIS IR mosaic, although not in the same projection, proved invaluable where image quality of the Viking mosaic is degraded. Contacts were transferred into ArcGIS to calculate surface areas for major material units, facilitating compilation of crater size-frequency statistics. Mapping methods herein draw on historical techniques (Gilbert, 1886; Wilhelms, 1972, 1990), as well as new mapping precedents set forth by geologic mappers in the terrestrial and planetary communities (Hansen, 1991; Tanaka and others, 1994; Hansen, 2000; Skinner and Tanaka, 2003; Tanaka and others, 2005).

The map area includes a variety of linear depressions and channel forms interpreted to be both the direct and indirect result of fluvial activity. Thus, terms like valley, channel, and canyon are all used extensively throughout this text. In general, the term “valley” typically applies to small elongate troughs, or systems of troughs, that appear to have formed by fluid flow but lack an obvious suite of bed forms on their floors. The term “channel” is in turn restricted to Martian troughs that display evidence of fluid flow (sinuosity, bed forms). “Canyon” is reserved for larger troughs that have relatively steep, scarp-like margins that may have been formed directly by fluid flow. For our purposes, we refer to Dao and Harmakhis Valles’ upper reaches, or heads, as canyons because they are relatively large in scale and do not preserve bed forms, nor do they resemble fluvial systems; however, the lower reaches and termini of Dao, Harmakhis, and Sungari Valles display varying degrees of fluvial landform preservation such that both channel and valley are used when discussing different locations of these complex systems.

Crater Counting Methodology

We derived relative age constraints for the geologic units in the eastern Hellas region in part by counting the number and size distribution of superposed impact craters within the areas of each major geologic unit (Tanaka, 1986; Tanaka and others, 1992). To examine statistics for craters ≥ 5 km in diameter, we imported the Martian crater database compiled by Barlow and others (2000) into ArcGIS. Evaluation of the Barlow crater database allowed us to (1) identify craters larger than 5 km within each mapped unit, (2) eliminate ridge rings, and (3) determine superposition on the surfaces of interest. We transferred unit boundaries into GIS using the Viking MTM and MOLA DEM bases, and surface areas were auto-calculated by ArcGIS 9.0 software; summing individual unit exposures provided cumulative unit areas. Table 1 summarizes the crater size-frequency distribution data for each major geologic unit; $N(5)$ and $N(16)$ represent the cumulative number of craters ≥ 5 and 16 km in diameter normalized to 1 million km^2 . The crater size-frequency error is $\pm(N^{0.5}/A) \times 10^6 \text{ km}^2$, where A = area. See figure 3 for a plot of the $N(5)$ and $N(16)$ crater data for major geologic units. We did not derive statistics for small areas or elongate exposures (vallis and channel units).

Stratigraphy

The four-MTM map area includes the terminal portions of Dao and Harmakhis Valles and their floor deposits, dissected plains materials, and deposits associated with the Hellas basin floor. We defined geologic units on our map to build from previous mapping (Price, 1998; Leonard and Tanaka, 2001; Mest and Crown, 2002) and on the results of our recent work on east Hellas rim geology (Crown and others, 2005). Following the mapping precedents of Leonard and Tanaka (2001) and Price (1998), materials in MTM quadrangles –40277, –45277, and –45272 (and –40272, previously mapped by Price, (1998)) are divided here into two major geologic assemblages: the Hellas

rim assemblage (three units) and the Hellas floor assemblage (three units). For most of the map area, the contact between these assemblages occurs at a prominent topographic break near the –5,800 m contour (fig. 2, red contour). At 1:5,000,000 scale, Leonard and Tanaka (2001) mapped materials within the region above –5,800 m as the Hesperian/Noachian dissected unit, member 1 (unit HNd_1), described as a rugged and heavily cratered material with relatively broad (several kilometer wide) smooth-floored channels and interpreted as older rim terrain that was extensively eroded and resurfaced by fluvial dissection and sedimentation. Below –5,800 m, they mapped materials as the Hesperian smooth interior material (unit His), described as an annular band of plains along the east margin of Hellas marked by smooth, locally undulating deposits that bury wrinkle ridges and have gradational boundaries to other interior floor materials. Mapping at 1:1,000,000 scale by Price (1998) subdivided the dissected material (rim assemblage) into the Hesperian/Noachian hummocky plains (unit HNh), which she described as irregular to highly irregular surfaces with a mottled appearance, and the Hesperian smooth plains (unit Hps), described as plains of slight to moderate relief cut by sinuous channels. She interpreted the hummocky plains as volcanic and sedimentary materials underlying the smooth plains, which are sedimentary deposits modified by fluvial and possibly periglacial and aeolian processes. The Price (1998) map area falls east of the rim/floor assemblage boundary, thus there was no evaluation of the floor assemblage in that study.

In addition to the rim and floor assemblages, we defined vallis and channel materials (seven units) and crater materials (three units). Leonard and Tanaka (2001) placed all vallis materials into one unit (AHv), which includes the heads, cavi, long sinuous depressions, and smooth floor deposits of Dao, Niger, Harmakhis, and Reull Valles, and interpreted it to be the result of catastrophic breakouts of groundwater and fluidized debris, followed by sapping and collapse. Price (1998) delineated several vallis units, for Dao Vallis in particular, recognizing multiple cut-off segments (units AHv_1 and AHv_2) and several units related to the continued evolution of the vallis systems (units AHvi , AHk , and AHv). Recent reevaluations of the geology of the circum-Hellas canyons suggest that at least the later stages in their evolution have been dominated by collapse, with the possibility that significant, catastrophic flooding may have been limited in scope and (or) been confined to early stages, evidence of which (streamlined islands, terraces) is not preserved in their current morphologies (Bleamaster and Crown, 2004; Crown and others, 2005).

Hellas Rim Assemblage

From THEMIS IR and VIS data, we have evaluated the contacts of units HNh and Hps mapped by Price (1998) and have extended these unit boundaries westward from MTM quadrangle –40272 to the boundary between the rim and floor assemblages. These two areally expansive units, which we redesignate units Nph and HNps , respectively, surround the distal portions of the Dao and Harmakhis Valles canyon

systems. The hummocky plains material (**Nph**) displays tens to hundreds of meters of relief and is located in the western part of the rim assemblage near its boundary with the floor assemblage and within high-standing inselbergs on the basin floor. Both THEMIS daytime and nighttime infrared images show a mottled and highly variable thermo-physical characteristic for unit **Nph** surfaces (fig. 4); visible data sets show that unit **Nph** has a lower albedo than the smooth plains of both the rim and floor assemblages. Unit **Nph** follows the regional slope of the eastern rim and is approximately bound by elevations $-5,200$ m and $-6,000$ m. Outcrops of unit **Nph** on the basin floor west of the rim/floor assemblage boundary express a similar elevation range, suggesting that these outcrops were once contiguous with the rim materials and have been locally preserved. Some outcrops of unit **Nph** display exposures over 400 m of continuous elevation change, providing a local thickness estimate of ~ 400 m; but the unit could be significantly thicker because its lower contact is not observed.

In MOC narrow-angle images, outcrops of finely layered materials are exposed atop local high-standing mesas, knobs, and surfaces near $-5,700 \pm 100$ m (fig. 5a); all identified exposures of layered outcrops (dot symbol on the map) are located within the boundaries of the hummocky plains material, based on a thorough search of all MOC narrow-angle images within a 20° by 20° area (lat 30° – 50° S., long 270° – 290° W.) (Crown and others, 2005). Layers appear as a fingerprint pattern in which successive layers make multiple-inset curvilinear benches whose outlines occur at similar topographic levels, indicating that they are most likely flat lying (fig. 5b,c). Correlation of layered beds from outcrop to outcrop was not possible without distinguishing marker beds, but the exposure, relation with elevation, and spatial concentration of the layered deposits within unit **Nph** suggest that the isolated layered outcrops most likely represent remnants of a once laterally extensive, and perhaps continuous, deposit that covered much of the east Hellas rim. These layers could represent the uppermost member of unit **Nph**, remnants of a more laterally extensive unit **HNps**, and (or) younger atmospherically derived, lacustrine, or fluvial sedimentary deposits. Because of the scale of the outcrops and the paucity of images that reveal the layers, the exact nature of the layered deposit is unclear. It probably is not dominated by young atmospheric mid-latitude mantling deposits, which would conform to local topography. More likely it is water-laid, either at the termini of Dao, Harmakhis, and other fluvial channels or in a Hellas-wide lake (Moore and Wilhelms, 2001, 2007; Crown and others, 2005; Wilson and others, 2007). Many additional scarps are present along the basin floor to the west; new high-resolution HRSC and HiRISE image data may help to identify additional layered outcrops and better constrain the regional distribution.

The smooth plains material (unit **HNps**) most likely consists of sedimentary deposits because it lacks visible lava-flow structures and displays a consistent smooth surface across a range of image resolution, with a few layered outcrops occurring at prominent scarps. The smooth plains superpose unit **Nph** and surround and contain several narrow, moderately sinuous, surface channels. In several places, these small channels appear as spaced and coalesced pits (indicative of immature develop-

ment) and (or) irregularly shaped depressions (possibly the result of modification of the original channel form). Some channel traces in unit **Nph** can be interpolated across gaps (probable windows) in unit **HNps** (lat 44° S., long 274° W.). This suggests that the channels were once through-going and that more progressive erosion has resulted in a transition into large, scarp-bound depressions present throughout unit **Nph** (lat 45° S., long 275° W.; lat 39.5° S., long 274° W.; and lat 40.0° S., long 272° W.). Although it is unclear if the smooth plains were deposited from the channels (bank-full deposits) or if the channels simply cut or undermine the plains, most likely both circumstances exist, and the small channels within the smooth plains likely represent the first stage in canyon development and hummocky-plains exposure (Crown and others, 2005). This is seen from truncation of the small channels by later channel and canyon development. Mobilization of the upper smooth plains materials and enlargement of the small channels into scarp-bound canyons would have occurred by downcutting from channels, scarp retreat and aeolian erosion, collapse from loss of volatiles, or a combination of these processes. Several zones within the smooth plains are in an initial stage of degradation and preserve original surface characteristics of the adjacent undisturbed plains (unit **HNps**); these areas include downdropped and rotated slump blocks and are shown with a stipple pattern, notably in the northeast quadrant of the map area adjacent to Dao Vallis (and along several sections of Dao, Niger, and Harmakhis Valles in the surrounding region). The small channels within unit **HNps** may have played an important role in the initial transportation of volatiles and volatile-rich sediments from the eastern Hellas highlands and in their redeposition as units **HNh** and **HNps**.

The age designations of both rim units mapped by Price (1998) are older on our map, based on our **N(5)** and **N(16)** values. A significantly greater areal exposure of the hummocky plains material in this map area has (1) increased the counting area and, thus, the precision of the count and (2) decreased the likelihood that a cover by younger deposits might contaminate counts. In addition, age designations based on **N(2)** values by Price (1998) may have been shifted away from the Noachian production slope by Amazonian surface processes, which more easily bury, degrade, and erode smaller craters. The new Noachian designation for the hummocky plains is consistent with the mostly Noachian designation of dissected unit 1 of Leonard and Tanaka (2001). **N(5)** counts for the smooth plains material within this study area are $\sim 33\%$ greater than in Price (1998) and result in our inclusion of Noachian in the unit's age designation; **N(16)** counts for the smooth plains (**Hps**) by Mest and Crown (2002) are in agreement with the older designation herein. The difference in counts, affecting only smaller crater diameters, may also be the result of Amazonian resurfacing (debris aprons, mid-latitude mantling), which is more concentrated east of the area mapped here.

In the southeast corner of the map area, the division between the rim and floor assemblages is a less distinct, more gradual transition than the sharp margin to the north; however, the $-5,800$ m contour still marks a significant morphologic change. The rim-floor assemblage contact manifests as a much less pronounced transition between the channeled plains (unit

AHpc, an expansive unit to the east; mapped by Mest and Crown, 2002, 2003) and the smooth interior floor material (unit **HNfis**). Some ridge traces cross this gradational boundary, suggesting that deformation either postdates deposition of unit **AHpc** or that ridges were in place and buried by unit **AHpc**; the subdued and smooth topography of ridges and lack of sharp embayment contacts support the latter. The surface of unit **AHpc** is smooth and displays several sinuous superposed channels; whereas, to the west, young superposed channels are lacking and several small to medium-sized craters mark a distinct morphologic difference, as apparent in crater counts (table 1). Channeled plains material is interpreted to be a sedimentary unit that formed following removal and redistribution of smooth plains material south of Reull Vallis located northeast of the map area. Unit **AHpc** may mark the westernmost floodplain deposits of Reull Vallis (Mest and Crown, 2002, 2003) or a possible older lacustrine deposit from a Hellas-wide lake; the present-day exposure likely represents the erosional retreat of materials that once continued farther west and into Hellas Planitia. Unit-age designation is consistent with counts of substantially larger areas to the east by Mest and Crown (2003) and suggests that significant aqueous reworking continued at least until the Late Hesperian.

Hellas Floor Assemblage

Hellas floor materials are moderately to heavily cratered, deformed by wrinkle ridges, and locally dissected or transected by the farthest extensions of Dao and Harmakhis Valles. Most of the floor assemblage in this map area is composed of smooth material (unit **HNfis**) with an undulating characteristic that forms clear and sharp embayment contacts and stratigraphic markers with unit **Nph** and ambiguous or gradational contacts when adjacent to rim assemblage unit **AHpc** and the various vallis units.

In the southeast quadrant of the map area, near the contact between units **HNfis** and **AHpc**, an anomalous zone of semi-exhumed craters exists (depicted on the map with a stipple pattern). Several of the crater rims within this zone merge with both the pronounced and the subdued morphologic features characteristic of Hellas Planitia regional deformation, namely wrinkle ridges. This spatial relation suggests that these craters predate the deformation rather than having coincidentally formed by impact at wrinkle-ridge intersections. This cratered zone appears to be a subsurface connection of ancient material between the hummocky plains on the rim and inselbergs on the floor that has been covered and later stripped, leaving behind a thin veil of unit **HNfis**. This substrate may represent extensions of unit **Nph** itself; however, the floor outcrops lie ~200 m below those on the rim. The substrate material may be a lower member of unit **Nph** or the original post-Hellas impact basement draped by unit **Nph**.

Near the mouth of Harmakhis Vallis, several scarp-bound plateaus preserve a wrinkle-ridge pattern like that in the anomalous crater zone and in high ground north and south of the sinuous depressions in unit **HNfis**. In this same region

several relatively deep sinuous depressions extend onto the Hellas floor and meander around high-standing plateaus. These distal extensions of Harmakhis Vallis may or may not represent genetic surface connections with the Harmakhis head valley to the northeast, because they do not preserve primary channel features linking their origins (Bleamaster and Crown, 2004); however, the characteristic plan-form shapes including sinuosity and braiding appear likely to be of fluvial origin (see Discussion). No wrinkle ridges are visible in the depressions, so the channel-like features postdate wrinkle-ridge deformation of the plateaus and the surrounding plains, both of which are resurfaced by unit **HNfis**, which predates significant downcutting of the Harmakhis Vallis terminus.

Within these depressions at the Harmakhis Vallis terminus, we identify two geologic units: hummocky floor material (unit **Hfh**) and smooth fill material (unit **AHfs**). Unit **Hfh** lies adjacent to and overlies the smooth interior floor material (unit **HNfis**) and broadens towards the basin center where the materials are dissected by several linear-curvilinear troughs. These troughs break the material into low-relief mesas and knobs (lat 42° S., long 278° W.). Materials of unit **Hfh** likely consist of Harmakhis paleochannel deposits, as well as materials mass wasted from the adjacent high-standing plateaus. The small-scale troughs may be remnants of paleodrainage or they may also be structural in nature, representing minor amounts of extension of a loosely consolidated sedimentary deposit. The deepest parts of these depressions, although discontinuous, may represent segments of the paleothalweg of the Harmakhis Vallis terminal channels. Unit **AHfs** lies in these lowest regions and has a gradational surface texture that is very smooth in its interior and hummocky near the contact with unit **Hfh**. This suggests that the unit has achieved sufficient thickness to more completely bury the hummocks of unit **Hfh** near the center of the paleochannel than at its edges. Unit **AHfs** is locally the youngest unit and has a plan-form characteristic like that of Quaternary alluvium along terrestrial river channels (contacts mimic topographic contours and deposits fill the lowest elevations of the channel), although unit **AHfs** may not be deposited as alluvial sediment. Complicating the interpretation of these depressions and their deposits are their subdued surface character and topography resulting from burial by as much as tens of meters of material by aeolian settling and (or) atmospheric frost-mantling deposits.

Vallis and Channel Materials

Several dozen small channels dissect the rim and floor assemblages. Most are depicted on the map with a blue line. Channel materials (**Hch₁**, **AHch₂**, and **AHch₃**), mapped in channels that have wide enough floors to warrant a unit designation, are composed of original channel deposits, eroded floor materials, materials mass-wasted from the walls, and any other subsequent fill materials. Crosscutting relations constrain the relative ages of the morphologic channel forms. On the basin rim, the small channels are located primarily within unit **HNps**. Most of these small channels are narrow, shallow, and

in general represent immature dissection; however, they reflect some of the oldest fluvial dissection of the rim when water may have been more prevalent on, or available to, the surface. Several channels parallel the larger vallis systems; when spatially coincident, small channels are truncated by younger, wider, and more developed canyons and valles. We also see examples of narrow, sinuous channels that contain segments that have been widened into a trough or small canyon. This relation, the discontinuous nature of some small channels, and the disrupted blocks along the margins of Dao and Harmakhis Valles favor an extended period of collapse and modification over a catastrophic, fluvial interpretation of the observed morphologies (Crown and others, 2005). Where the canyons are sufficiently wide, Amazonian or Hesperian valley fill superposes their floors (units AHV_D and AHV_S). Floor materials are composed of remnants of surrounding plains materials mixed with younger aeolian, mass-wasted, and mantling materials. These materials display isolated pits of various sizes and lineations parallel to canyon walls. The pits do not appear to be impact craters (no ejecta), thus they must be related to collapse over void space. This suggests that the materials have been volatile-rich and (or) have significant porosity and that collapse occurs when volatiles migrate out of the sediments. Volatile-rich material (sediments with interstitial ice) is also consistent with the floor lineations, which indicate some component of flow, in successive downcanyon and (or) across-canyon events. Mantling deposits on canyon walls flow into and merge with floor materials in some places, which is again consistent with both cross-canyon and downcanyon movement.

The largest, most mature, canyon segments of Dao/Niger and Harmakhis Valles, which also dissect the rim and floor assemblages, are thought to be more highly evolved features: zones where continued and possibly concentrated surface flow, subsurface flow and piracy, and volatile migration have served to widen the once-narrow surface channels. The lower reaches of Dao Vallis preserve several episodes of channel development showing abandoned truncated channels (units Hc₁ and AHc₂) (fig. 6) and provide evidence of a protracted history contrary to a single catastrophic mechanism for Dao and Harmakhis Valles development.

With the exception of a lobe extending from the mouth of Dao Vallis (unit AHV_t), distinct depositional margins are lacking near channel and canyon mouths that cross the rim-floor assemblage boundary. Unit AHV_t ranges upward from a few to tens of kilometers in width with subparallel margins and is entrenched by a channel nearly down the center of its length (fig. 7). The resultant deposit's morphology is more consistent with emplacement in a single event rather than successive individual flows; channel entrenchment may represent waning of material transport or subsequent dissection.

Crater Materials

One hundred and twenty craters, ranging from a few kilometers to 40 km in diameter, buried and exposed, have been identified and marked with a crater-rim symbol. Of these,

56 (mostly with diameters ≥ 5 km), including Bogia crater, have associated ejecta materials, floor materials, and (or) peak materials. Three unit designations are used to differentiate crater peak material (unit cp), crater undivided material (unit cu), and crater fill (unit cf). Bogia crater (lat 44.7° S., long 276.6° W.; 39.4 km diameter) contains all three crater units and is the only crater in the region with a central peak typical of larger impact craters. Several craters have floor deposits (unit cf), which may be mass-wasted material from the crater rim, atmospheric deposits, lacustrine sediments, or a combination of all of these. Several crater walls are dissected by young hillside gullies; no deltaic landforms have been identified in any of these craters.

South of the Harmakhis Vallis terminal plateau region, several adjacent craters display commingled ejecta blankets, which have radial lineations, lobate margins, and dark ejecta (Viking and THEMIS IR datasets). A variety of degradation states is evident and consistent with various ages of the formative impacts; however, the exposed surface is dominated by armored ejecta blankets with few superposed pristine craters, suggesting that this surface was buried and has since been exhumed in a relatively uniform manner. Craters whose ejecta blankets include the dark material (cross-hatch pattern) are interpreted to have excavated rocks from unit Nph, which lies beneath unit HNFis and also displays a low albedo.

Discussion

This geologic study has shed light on the role of water in the evolution of Hellas Planitia and the Martian surface, including the possibility of ancient lake deposits hypothesized for western Hellas. Geomorphic and geologic evidence reveals an extended history of widespread fluvial dissection, but evidence of large-scale catastrophic flooding, as in the circum-Chryse Planitia outflow channels, is lacking, either because it never occurred or it occurred earlier and has since been destroyed.

Fluvial Systems that dissect the Hellas Rim

The eastern Hellas rim has experienced fluvial activity throughout its long history. A progression from small ancient channels that dissect the highland terrains to massive canyon development and to contemporary gullies on the slopes of crater and canyon walls is preserved. Timing relations along segments of Dao and Harmakhis Valles place the major development of these valles in the middle of the protracted history.

The geology of the eastern rim of Hellas basin, and in particular the sequence of plains materials surrounding Dao and Harmakhis Valles, suggest the formation of a depositional shelf that largely covers any remnant highland terrains previously preserved here. Widespread dissection along vallis and channel systems is evident on the basin rim. The following idealized stages can account for the observed geologic relations: (1) deposition of sedimentary layers possibly with interbedded volcanics, (2) strata enriched with volatiles either during deposition or subsequently, (3) small-scale surface and subsurface pathways established through rim materials to the basin floor,

(4) plains strata fractured and lowered along these pathways, partly because of weakening by volatile migration, (5) blocks subsided and rotated by continued collapse and fracturing, (6) volatile infiltration facilitated by the resultant irregular topography, leading to growth of sapping valleys along fractures and over subsurface voids, (7) collapse of canyon walls and localized erosion of wall materials, and (8) resurfacing of canyon floors and mass-wasted deposits from canyon walls and lineated valley-fill deposits extending downcanyon and surrounding remnant hills and mounds of collapsed plains.

The canyons may have developed either in a regional episode of subsidence or in distinct episodes of initial subsidence and collapse at different times in different places. Topographic coincidence of canyon heads with the $-1,800$ m contour (see Crown and others, 2005) supports a common origin, possibly by the lowering of a lake level or by commonalities in the subsurface geology. Local factors may affect subsequent morphologic development in either scenario. Eventually the entire eastern Hellas landscape, as well as regions south and north of 40° latitude, preserves morphologies consistent with surface and subsurface ice-dominated environments. We propose that Dao and Harmakhis Valles are the most evolved channel features in a suite of channels on the rim; their floors are among the youngest of the channel and vallis deposits including the tongue of material that extends from Dao Vallis' terminus onto the Hellas floor.

Extensions of Dao and Harmakhis Valles onto the Basin Floor and Contributions to Hellas Planitia from the Rim

Direct connections between the Hellas floor materials and their potential rim sources are difficult to identify (except for the small lobe at the mouth of Dao Vallis). Alternatively, the eastern Hellas floor materials (1) may be composed of far-reaching deposits from Dao and Harmakhis Valles, extending west of the map area, or (2) may consist of planitia-wide deposits mostly of local origin and not delivered by Dao and Harmakhis Valles. Amazonian resurfacing (aeolian infill, mid-latitude mantling) apparently has masked any original relations between canyon-floor and Hellas-floor materials. Direct comparison of vallis and canyon-cavity volumes (Dao, Niger, Harmakhis, and Reull Valles) (Mest, 1998; Tanaka and Leonard, 1995) to the estimated total volume of sediment contained in the eastern Hellas floor deposit showed that missing material from the four major tributaries accounts for only a small fraction of the material present on the floor (Rogey and others, 2003). In any case, the small channels and larger valles were likely significant paleopathways for the migration from the rim to the floor of liquid water, debris-rich slurries, or glacial flows. The volumes of volatiles and sediments that may have been transported from, or through, the rim to the basin floor remains uncertain (Crown and others, 2005). Similarly, marine canyons on Earth show little correlation between the size of the canyon, the sedimentary flux, and the final volume of their associated deposits (as high as 1 to 3 orders of magnitude greater sediment transport) (Normark and Carlson, 2003), thus it is not surprising for the Martian values to remain unconstrained.

Boundary between the East Hellas Basin Rim and Hellas Planitia

Both the Hellas rim and floor assemblages contain units of Noachian, Hesperian, and Amazonian age. In each case the Noachian materials appear to have been exposed by erosion following significant burial by younger materials. In each situation, Amazonian surface processes are masking critical relations between Noachian and Hesperian materials. Key to constraining the age of the rim-floor boundary to a minimum of Hesperian is that the large vallis filled by later materials (AHv_D and AHv_H) cut directly across the contact. However, the nature of the rim-assemblage materials, in particular unit Nph, may push the boundary's age back into the Noachian. The characteristic of the rim/floor boundary located at $-5,800$ m is crucial to its interpretation. This topographic level in the eastern region marks a distinct variation in rim morphology. The $-5,800$ m contour deflects inward toward the basin center precisely where Dao and Harmakhis Valles enter the Hellas floor. Several outcrops of the finely layered deposits of unit HNps also occur here. The deflection of the contour coupled with the presence of the layered materials strongly suggests that this area is a site of concentrated (relative to other regions around the basin) and significant deposition within the Hellas basin interior. After considerable reconnaissance and analysis of the Hellas rim (see Crown and others, 2005), we are confident that this deposit is unique to eastern Hellas and is most likely the result of concentrated aqueous activity (precipitation, recharge, storage and release of volatiles) related to persistent atmospheric circulation patterns that allow for migration of volatiles from the southern pole (models by Colaprete and others, 2004, 2005). The availability of volatiles in this location facilitates both weathering and mobilization of the highland materials from the rim to the floor of Hellas. We suggest that this present-day shelf is a volatile-rich accumulation zone (both ancient and contemporary). The margin preserved at $-5,800$ m may represent a lake highstand or the extent of an ice-covered body of water (Moore and Wilhelms, 2001, 2007). If unit Nph represents an early phase of this depositional shelf, then the rim materials were beginning to build out onto the floor of Hellas in the Noachian with later deposits of smooth plains in the Hesperian, which may or may not be associated with unit Nph; if a basin-wide lake did exist at this time, then materials being shed from the eastern rim may have been deposited subaqueously as deltaic sequences, which would be interbedded with lacustrine sediments from the basin as a whole. If the Hellas lake was ice covered, materials may have been deposited as they were shed from the eastern rim and abutted against an ice margin.

With respect to later modification of the material on the eastern rim (Dao and Harmakhis Valles), if the volatile-rich depositional shelf existed as described above, it would have facilitated collapse and growth of the large canyon systems by supplying unconsolidated materials with high infiltration capacities, sufficient volatile components, and pathways for easy removal. Additional factors that may have contributed to eastern Hellas' unique geology are its proximity to both Hadriaca Patera, a potential heat source providing enhanced geothermal flow from magma bodies and surface flows, and southern hemi-

sphere atmospheric circulation, which carries volatile components directly off the southern polar cap and emplaces them east of Hellas basin.

Geologic History

The following sequence of events is suggested from the geologic, geomorphic, and topographic relations in the mapped part of eastern Hellas basin:

1. Formation of Hellas basin and the circum-Hellas highlands during the Early Noachian Epoch provides the topographic framework for subsequent geologic activity.

2. Degradation and removal of material throughout the Noachian from the basin rim results in a significant topographic depression in a northeastern corridor between Hellas Planitia and Hesperia Planum northeast of the map area; this represents a period of erosion and transport and a significant gap in the geologic record within the map area.

3. Materials shed from the Hellas rim are locally deposited around high-standing knobs of the degraded rim (unit **Nph**). This unit represents remnants of the ancient highlands and may include pre-Hellas crust, contributions from the Hellas impact (melt sheet, ejecta, shocked basement), and post-Hellas impacts (including Argyre impact ejecta) intermixed with younger sediments. The anomalous zone of craters (stipple pattern in unit **HNfis**) on the Hellas floor also represents a remnant Noachian surface that was buried and later exhumed.

4. Widespread deposition of plains on the rim and floor (units **Nph**, **HNps**, and **HNfis**). These materials may have been deposited subaqueously in a standing body of water or along the margin of an ice-covered lake (Moore and Wilhelms, 2001, 2007; Crown and others, 2005). If the sequence of plains exposed in units **Nph** and **HNps** (above $-5,800$ m) is even partially lacustrine in nature, then extensive Hellas paleolakes may have existed into the Early Hesperian Epoch; however, if not, then Hellas paleolakes would have been more ancient and (or) constrained to the Hellas basin floor.

5. Fluvial dissection becomes prominent on the east rim of the Hellas basin in the Hesperian Period, perhaps in relation to recession of Hellas paleolakes. Small-scale channels develop within and dissect unit **HNps**' surface and transport material toward Hellas Planitia. It is likely that the larger valleys evolved from some of these smaller channels, thus the early development of Dao and Harmakhis Valles would have begun in the Early Hesperian Epoch.

6. Deformation in the form of northwest-trending wrinkle ridges crosscuts the deposits of Hellas Planitia (unit **HNfis**). This deformation postdates widespread Hellas paleolakes (stands near $-5,800$ m) and could have formed by rebound of the lithosphere in response to removal of the overburden of water or ice, but it predates the intermediate stages of Dao and Harmakhis development (especially at their termini: units **Hfh** and **AHvt**), signifying that there was glacial or fluvial activity along the eastern rim well into the Late Hesperian and possibly Early Amazonian Epochs.

7. Widespread channel development transitions to localized enlargement of channel segments by sapping and collapse

(stipple zone in unit **HNps**) facilitated by earlier deposited sedimentary and volcanic materials (units **Nph** and **HNps**).

8. Deposition of plains materials (unit **AHpc**) from Reull Vallis overflow (Mest and Crown, 2002, 2003) and (or) ice-rich surface mantles were followed by dissection by channels via sheet wash and scour in the southern portion of the map area.

9. Vallis floor materials (units **AHfs**, **AHv_D**, **AHv_H**, and **AHv_S**) and channel deposits (units **Hc₁**, **AHc₂**, and **AHc₃**) may span a significant amount of time depending on the specific source of the material. Downcanyon contributions sourced from the canyon heads may begin to collect concurrently with development of the canyons in the Early Hesperian Epoch, whereas wall contributions via localized mass wasting may have been supplied into the Late Amazonian Epoch.

10. Craters within this region likely formed throughout the preserved geologic record and exhibit a range of preservation states; the complex surface morphologies observed may be attributed to various combinations of crater size and age along with different degrees of crater burial and exhumation. Craters with the dark ejecta (within unit **HNfis**) are most likely the result of younger impact events that have excavated the underlying ancient basement material of unit **Nph**.

11. The Amazonian Period is characterized by the local exhumation and redistribution (aeolian dominated) of materials and continued exposure of hummocky plains on the rim (unit **Nph**) and floor (unit **Hfh**) of Hellas Planitia. Widespread deposition of mid-latitude mantling deposits in southernmost latitudes, the formation of gullies on crater and canyon walls, and the development of wind and slope streaks (mostly small components of vallis and channel materials) most likely formed over several episodes of activity in the recent geologic past; several of these small, young morphologic features are not mapped (see Bleamaster and Crown, 2005, for gully and mantle morphologies).

Acknowledgments

The authors wish to thank Katherine Price and Don Wilhelms for thorough and insightful reviews, Ken Tanaka for his continued service to the planetary geologic mapping community as map coordinator, Jenny Blue for her assistance with planetary nomenclature, and Jan Zigler and Darlene Ryan for their editing and graphical expertise, respectively. This work was made possible by funding from NASA's Planetary Geology and Geophysics program (Geologic Investigations of the Martian Highlands, grant #NNG04GI85G). This is Planetary Science Institute contribution #448.

References Cited

- Baker, V.R., Strom, R.G., Gulick, V.C., and 3 others, 1991, Ancient oceans, ice sheets, and the hydrological cycle on Mars: *Nature*, v. 352, p. 589–594.
- Barlow, N.G., Boyce, J.M., Costard, F.M., and 6 others, 2000, Standardizing the nomenclature of Martian impact crater

- ejecta morphologies: *Journal of Geophysical Research*, v. 105, p. 26733–26738.
- Berman, D.C., Crown, D.A., and Bleamaster, L.F., III, 2009, Degradation of mid-latitude craters on Mars: *Icarus*, v. 200, p. 77–95 (doi:10.1016/j.icarus.2008.10.026).
- Berman, D.C., Hartmann, W.K., Crown, D.A., and Baker, V.R., 2005, The role of arcuate ridges and gullies in the degradation of craters in the Newton Basin region of Mars: *Icarus*, v. 178, p. 465–486.
- Bleamaster, L.F., III, and Crown, D.A., 2004, Morphologic development of Harmakhis Vallis, Mars, in *Lunar and Planetary Science Conference XXXV: Houston, Lunar and Planetary Institute, Abstract 1825 [CD-ROM]*.
- Bleamaster, L.F., III, and Crown, D.A., 2005, Mantle and gully associations along the walls of Dao and Harmakhis Valles, Mars: *Geophysical Research Letters*, v. 32, p. L20203 (doi:10.1029/2005GL023548).
- Carr, M.H., 1996, *Water on Mars*: London, Oxford University Press, 228 p.
- Chuang, F.C., and Crown, D.A., 2005, Surface characteristics and degradational history of debris aprons in the Tempe Terra/Mareotis Fossae region, Mars: *Icarus*, v. 179, p. 24–42 (doi:10.1016/j.icarus.2005.05.014).
- Colaprete, A., Haberle, R.M., Segura, T.L., Toon, O.B., and Zahnle, K., 2004, The effects of impacts on the early Martian climate, in *Second conference on early Mars—Geologic, hydrologic, and climatic evolution and implications for life*: Houston, Lunar and Planetary Institute, Abstract 8016 [CD-ROM].
- Colaprete, A., Barnes, J.R., Haberle, R.M., and 3 others, 2005, Albedo of the south pole on Mars determined by topographic forcing of atmosphere dynamics: *Nature*, v. 435, p. 184–188.
- Crown, D.A., and Greeley, R., 1993, Volcanic geologic map of Hadriaca Patera and the eastern Hellas region of Mars: *Journal of Geophysical Research*, v. 98, no. 02, p. 3431–3451.
- Crown, D.A., and Greeley, R., 2007, Geologic map of MTM –30262 and –30267 quadrangles, Hadriaca Patera region of Mars: U.S. Geological Survey Scientific Investigations Map SIM 2936.
- Crown, D.A., Bleamaster, L.F., III, and Mest, S.C., 2005, Styles and timing of volatile-driven activity in the eastern Hellas region of Mars: *Journal of Geophysical Research*, v. 110, no. E12S22 (doi:10.1029/2005JE002496).
- Crown, D.A., Price, K.H., and Greeley, R., 1992, Geologic evolution of the east rim of the Hellas basin, Mars: *Icarus*, v. 100, p. 1–25.
- Crown, D.A., Bleamaster, L.F., III, Mest, S.C., and Teneva, L.T., 2005, Styles and timing of volatile-driven activity in the eastern Hellas region of Mars, in *Lunar and Planetary Science Conference XXXVI: Houston, Lunar and Planetary Institute, Abstract 2097 [CD-ROM]*.
- Gilbert, G.K., 1886, Inculcation of scientific method: *American Journal of Science*, v. 31, no. 284–298.
- Greeley, R., and Crown, D.A., 1990, Volcanic geology of Tyrrhena Patera, Mars: *Journal of Geophysical Research*, v. 95, p. 7133–7149.
- Greeley, R., and Guest, J.E., 1987, Geologic map of the eastern equatorial region of Mars: U.S. Geological Survey Miscellaneous Investigations Series Map I–1802–B.
- Greeley, R., and Spudis, P.D., 1981, Volcanism on Mars: *Reviews of Geophysics*, v. 19, p. 13–41.
- Greeley, R., Lancaster, N., Lee, S., and Thomas, P., 1992, Martian aeolian processes, sediments, and features, in Kieffer, H.H., Jakosky, B.M., Snyder, C.W., and Matthews, M.S., eds., *Mars*: Tucson, University of Arizona Press, p. 730–766.
- Hansen, V.L., 2000, Geologic mapping of tectonic planets: *Earth and Planetary Science Letters*, v. 176, p. 527–542.
- Hansen, W.R., ed., 1991, *Suggestions to authors of the reports of the United States Geological Survey, Seventh Edition*: Washington, D.C., U.S. Government Printing Office, 289 p.
- Kargel, J.S., and Strom, R.G., 1992, Ancient glaciation on Mars: *Geology*, v. 20, p. 3–7.
- Leonard, G.J., and Tanaka, K.L., 2001, Geologic map of the Hellas region of Mars: U.S. Geological Survey Geologic Investigations Series Map I–2694.
- Leverington, D.W., and Ghent, R.R., 2004, Differential subsidence and rebound in response to changes in water loading on Mars—Possible effects on the geometry of ancient shorelines: *Journal of Geophysical Research*, v. 109, no., E01005 (doi:10.1029/2003JE002141).
- Lucchitta, B.K., 1984, Ice and debris in the fretted terrain, Mars, in *Proceedings of Lunar and Planetary Science XIV: Journal of Geophysical Research*, v. 89, p. B409–B418.
- Mest, S.C., 1998, *Geologic History of the Reull Vallis region, Mars*: Penn., University of Pittsburgh, Masters Thesis, 269 p.
- Mest, S.C., and Crown, D.A., 2001, Geology of the Reull Vallis region, Mars: *Icarus*, v. 153, p. 89–110.
- Mest, S.C., and Crown, D.A., 2002, Geologic map of MTM –40252 and –40257 quadrangles, Reull Vallis region of Mars: U.S. Geological Survey Geologic Investigations Series Map I–2730.
- Mest, S.C., and Crown, D.A., 2003, Geologic map of MTM –45252 and –45257 quadrangles, Reull Vallis region of Mars: U.S. Geological Survey Geologic Investigations Series Map I–2763.
- Mest, S.C., and Crown, D.A., 2006, Geologic map of MTM –20272 and –25272 quadrangles, Tyrrhena Terra region of Mars: U.S. Geological Survey Geologic Investigations Series Map I–2763.
- Moore, J.M., and Edgett, K.S., 1993, Hellas Planitia, Mars—Site of net dust erosion and implications for the nature of basin floor deposits: *Geophysical Research Letters*, v. 20, p. 1599–1602.
- Moore, J.M., and Wilhelms, D.E., 2001, Hellas as a possible site of ancient ice-covered lakes on Mars: *Icarus*, v. 154, p. 258–276.
- Moore, J.M., and Wilhelms, D.E., 2007, Geologic map of part of western Hellas Planitia, Mars: U.S. Geological Survey Geologic Investigations Series Map I–2953.
- Morrison, S.J., and Frey, H.V., 2007, Crater densities in Noachis Terra—Evidence for overlapping ejecta from Argyre

- and Hellas, *in* Lunar and Planetary Science Conference XXXVIII: Houston, Lunar and Planetary Institute, Abstract 1355 [CD-ROM].
- Mustard, J.F., Cooper, C.D., and Milliken, R.E., 2001, Evidence for recent climate change on Mars from the identification of youthful near-surface ground ice: *Nature*, v. 412, p. 411–414.
- Mustard, J.F., Thollet, P., Murchie, S.L., 10 others, and the CRISM science team, 2007, OMEGA-CRISM characterization of phyllosilicates: Lunar and Planetary Institute, Seventh International Conference on Mars, abstract #3230.
- Normark, W.R., and Carlson, P.R., 2003, Giant submarine canyons—Is size any clue to their importance in the rock record?: Geological Society of America, Special Paper 370, 15 p.
- Pelkey, S.M., Mustard, J.F., Murchie, S., 8 others, and the CRISM science team, 2007, CRISM observations of hydrated crater deposits in Terra Tyrrhena, Mars *in* Lunar and Planetary Science Conference XXXVIII: Houston, Lunar and Planetary Institute, Abstract 1994 [CD-ROM].
- Peterson, J.E., 1977, Geologic map in Noachis quadrangle of Mars: U.S. Geological Survey Miscellaneous Investigations Series Map I-910.
- Peterson, J.E., 1978, Volcanism in the Noachis-Hellas region of Mars, 2, *in* Proceedings of Lunar and Planetary Science Conference, 9th: Houston, Lunar and Planetary Institute, p. 3411–3432.
- Pierce, T.L., and Crown, D.A., 2003, Morphologic and topographic characteristics of debris aprons in the eastern Hellas region, Mars: *Icarus*, v. 163, p. 46–65 (doi:10.1016/S0019-1035(03)00046-0).
- Potter, D.B., 1976, Geologic map of the Hellas quadrangle of Mars: U.S. Geological Survey Miscellaneous Investigations Series Map I-941.
- Price, K.H., 1998, Geologic map of MTM -40262, -40267, and -40272 quadrangles, Dao, Harmakhis and Reull Valles region of Mars: U.S. Geological Survey Miscellaneous Investigations Series Map I-2557.
- Rogero, I.M., Raitala, J., Aittola, M., and Kostama, V.-P., 2003, Estimated volumes of Dao, Niger, Harmakhis, and Reull Vallis and the deposits inside Hellas basin: Vernadsky-Brown Micro symposium 38, MS065.
- Schultz, P.H., 1984, Impact basin control of volcanic and tectonic provinces on Mars, *in* Lunar and Planetary Science Conference, XV: Houston, Lunar and Planetary Institute, p. 728–729.
- Schultz, R.A., and Frey, H.V., 1990, A new survey of large multiring impact basins on Mars: *Journal of Geophysical Research*, v. 95, p. 14,175–14,189.
- Scott, D.H., and Carr, M.H., 1978, Geologic map of Mars: U.S. Geological Survey Miscellaneous Investigations Series Map, I-1083.
- Seidelmann, P.K., Abalakin, V.K., Bursa, M., and 8 others, 2002, Report of the IAU/IAG working group on cartographic coordinates and rotational elements of the planets and satellites: *Celestial Mechanics and Dynamics of Astronomy*, v. 82, p. 83–110.
- Skinner, J.A., Jr., and Tanaka, K.L., 2003, How should planetary map units be defined?, *in* Lunar and Planetary Science Conference XXXIV: Houston, Lunar and Planetary Institute, Abstract 2100 [CD-ROM].
- Squyres, S.W., 1979, The distribution of lobate debris aprons and similar flows on Mars: *Journal of Geophysical Research*, v. 84, p. 8087–8096.
- Squyres, S.W., 1989, Urey prize lecture—Water on Mars: *Icarus*, v. 79, p. 229–288.
- Squyres, S.W., and Carr, M.H., 1986, Geomorphic evidence for the distribution of ground ice on Mars: *Science*, v. 231, p. 249–252.
- Squyres, S.W., Wilhelms, D.E., and Moosman, A.C., 1987, Large-scale volcano-ground ice interactions on Mars: *Icarus*, v. 70, p. 385–408.
- Squyres, S.W., Clifford, S.M., Kuzmin, R.O., Zimbelman, J.R., and Costard, F.M., 1992, Ice in the martian regolith, *in* Kieffer, H.H., Jakosky, B.M., Snyder, C.W., and Matthews, M.S., eds., Mars: Tucson, University of Arizona Press, p. 523–554.
- Tanaka, K.L., 1986, The Stratigraphy of Mars *in* Proceedings of Lunar and Planetary Science Conference 17, Part 1: *Journal of Geophysical Research Supplement* 91, p. E139–158.
- Tanaka, K.L., and Leonard, G.J., 1995, Geology and landscape evolution of the Hellas region of Mars: *Journal of Geophysical Research*, v. 100, p. 5407–5432.
- Tanaka, K.L., Scott, D.H., and Greeley, R., 1992, Global Stratigraphy, *in* Kieffer, H.H., Jakosky, B.M., Snyder, C.W., and Matthews, M.S., eds., Mars: Tucson, University of Arizona Press, p. 345–382.
- Tanaka, K.L., Skinner, J.A., and Hare, T.M., 2005, Geologic map of the northern plains of Mars: U.S. Geological Survey Scientific Investigations Map 2888, scale 1:15,000,000.
- Tanaka, K.L., Kargel, J.S., MacKinnon, D.J., Hare, T.M., and Hoffman, N., 2002, Catastrophic erosion of Hellas basin rim on Mars induced by magmatic intrusion into volatile-rich rocks: *Geophysical Research Letters*, no. 29 (doi:10.1029/2001GL013885).
- Tanaka, K.L., Moore, H.J., Schaber, G.G., and 9 others, 1994, The Venus geologic mappers' handbook: U.S. Geological Survey Open-File Report 94-438, 50 p.
- Wilhelms, D.E., 1972, Geologic mapping of the second planet: U.S. Geological Survey Interagency Report, Astrogeology 55, 36 p.
- Wilhelms, D.E., 1990, Geologic mapping, *in* Greeley, R., and Batson, R.M., eds., Planetary Mapping: New York, Cambridge University Press, p. 208–260.
- Wilson, S.A., Howard, A.D., Moore, J.M., and Grant, J.A., 2007, Geomorphic and stratigraphic analysis of crater Terby and layered deposits north of Hellas basin, Mars: *Journal of Geophysical Research*, v. 112, no. E08009 (doi:10.1029/2006JE002830).

Table 1. Areas, crater densities, relative ages, and contact relations for map units in the eastern Hellas Planitia region of Mars.

Unit Name	Unit Symbol	Area (km ²)	Count ¹ N(5)	Count ¹ N(16)	N(5) ²	N(16) ²	N(5) Epoch range	N(16) Epoch range	Designation ³	Contact Relations		
										Younger than	Overlaps in time	Older than
Channeled plains material	AHpc	34,370	2	0	58±41	--	LH-EA		LH-EA	Nph, HNps, HNfis		
Hummocky floor material	Hfh	16,463	2	0	121±86	--	LN-EA		H	Nph, HNfis		AHfs
Smooth interior floor material	HNfis	136,790	25	4	183±37	29±15	LN-EH	LN-EH	LN-EH	Nph	AHv _H , AHv _D , AHv _S	Hfh, AHfs, AHpc, AHv _t
Smooth plains material	HNps	68,463	12	0	175±33	--	LN-EH		LN-EH	Nph		Hc ₁ , AHc ₂ , AHv _H , AHv _D , AHv _S
Hummocky plains material	Nph	72,402	23	5	318±66	69±31	LN	LN	LN			HNfis, HNps, Hfh, Hc ₁ , AHc ₂ , AHv _H , AHv _D , AHv _S

¹ Actual number of craters counted within the unit area.

² N(x), No. craters >x km in diameter per 10⁶ km²; error, ± [(N^{1/2})/A] x 10⁶ km².

³ Unit age designation determined by superposition relations and crater density analysis; N, Noachian; H, Hesperian; A, Amazonian; E, Early; L, Late (Tanaka, 1986).